4. S. S. Kutateladze and A. I. Leont'ev, Heat and Mass Transfer and Skin Friction in Turbulent Boundary Layer [in Russian], Énergiya, Moscow (1972).
5. G. A. Grigor'ev, E. G. Zaulichnyi, V. Ya. Ivanov, and G. B. Trubachev, "Supersonic flow in variable cross-section channel with separated regions," in: Investigation of Wall Layers of Viscous Fluid [in Russian], Inst. Teor. Prikl. Mekh., Sib. Otd. Akad. Nauk SSSR, Novosibirsk (1979).
6. E. P. Dyban and É. Ya. Épik,"Microstructure of boundary layer and transfer processes in them at high turbulence levels of the outer film," in: Proceedings of XVIII Sibir. Teplofiz. Sem., Part II, Inst. Teplo. Fiz., Sib. Otd. Akad. Nauk SSSR, Novosibirsk (1975).
7. A. Slanciauskas and J. Ziugzda, "Regelmäßige Wirbelstrukturen und Warmeübertragungsprozesses," in: Tagung Transportprozesse in Turbulenten Strömungen, Vortrage-Heft III, Berlin (1979).
8. G. S. Settles, D. R. Williams, et al., "Mixing of free turbulent shear layer in compressible fluid," Raketn. Tekh. Kosmonavt., 20, No. 2 (1982).
9. K. K. Horstman, G. S. Settles, et al., "Mixing free shear layer in compressible turbulent flow," Raketn. Tekh. Kosmonavt., 20, No. 2 (1982).
10. M. G. Ktalkherman, "Investigation of separated flows in channel (structure and heat transfer)," Synopsis of Candidate Thesis, Inst. Teor. Prikl. Mekh., Sib. Otd. Akad. Nauk SSSR, Novosibirsk (1971).
11. É. P. Volchkov, V. P. Lebedev, and A. N. Yadykin, "Heat transfer at off-design conditions in Laval nozzle with fluid certain," in: Heat and Mass Transfer VI, Vol. 1, Part 1, Minsk (1980).

PROPERTIES OF THE INTERACTION OF INTERFERENCE AND DIFFRACTION FLOWS AT SUPERSONIC VELOCITIES

M. D. Brodetskii, A. I. Maksimov, and A. M. Kharitonov

UDC 533:6.011:532.526.5

When supersonic flow takes place past angular configurations at angles of attack and slip, a number of interference and diffraction phenomena are observed. Up to now, adequate theoretical [1-10] and experimental [2, 11-22] studies have been performed only on isolated interference and diffraction flows which take place when there is longitudinal flow past an interior or exterior dihedral angle formed by the intersection of plane surfaces.

However, cases of mixed interaction between interference and diffraction flows, which take place, for example, when there is flow past the regions of adjunction of various elements of aircraft, are often encountered in practice. The known theoretical solutions of analogous problems in the linear formulation [1, 3] do not take account of some properties of the real flow. It is therefore of great interest to conduct experimental investigations of such flows on schematized models.

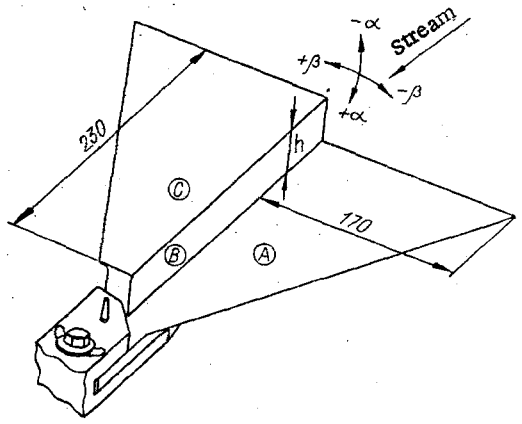

Fig. 1

Novosibirsk. Translated from Zhurnal Prikladnoi Mekhaniki i Tekhnicheskoi Fiziki, No. 1, pp. 106-116, January-February, 1986. Original article submitted October 29, 1984.

 0021-8944/86/2701-0094$12.50

The model of a plate with a longitudinal step (Fig. 1) includes an interior and exterior dihedral angle, which we shall provisionally call the angles of interference and diffraction. Experimental investigations on the visualization of the stream were conducted in the T-313 with tunnel of the Institute of Theoretical and Applied Mechanics, Siberian Branch, Academy of Sciences of the USSR, over a wide range of variation of the angles of attack and slip at Mach numbers of $M_\infty = 2.27$, 3, and 4 and Reynolds numbers of $Re \approx 26 \cdot 10^6$, $34 \cdot 10^6$, and $52 \cdot 10^6$ (for a characteristic dimension of 1 m). The height h of the longitudinal step was varied from 12.5 to 50 mm.

Positive angles of attack and slip of the model corresponded to compression flows, and negative angles to rarefraction flow. The errors in the determination setting of the angles α and β did not exceed $\pm 0.1°$, and the errors in the determination of the angles of inclination of the separation lines and reattachment lines of the stream from the pictures of the limiting streamlines did not exceed ±2°.

Most of the experiments were conducted with natural development of the boundary layer on the faces of the model. From estimates based on the results of oil-and-carbon-black visualization and on direct measurements of the minimum and maximum pressure transition after a direct jump on a flat plate, the region of transition from the laminar to the turbulent boundary layer is found to lie 25-130 mm from the leading edge of the model. As M_∞ increases, the transition zone moves backward. However, near the rib of the interior angle the transition takes place immediately around the leading edge of the model [23].

According to the data of [3, 24], the most interesting zone for our investigations lies between the limits of 2.5 and 4 provisional calibers, $x_h = h \cot \alpha_0$, from the leading edge, where h is the height of the longitudinal step, α_0 is the Mach angle for an unperturbed stream. In the front part of the model ($x \leqslant 0.5x_h$) we observe the same phenomena as in the case of flow past isolated dihedral angles, but they are affected to a large extent by the state of the boundary layer on the faces and are not always repeatable.

On a plate with a longitudinal step, depending on the angles of attack and slip, several characteristic types of flow may take place.

1. When the slip angle is $\beta = 0$, the leading edge of the vertical face induces only weak perturbations, which are due to its finite thickness, and the flow situation is completely determined by the intensity of the condensation jumps from the upper and lower faces, i.e., by the angle of attack of the model. As the angle of attack α increases, there is an increase in the pressure drops at the shock waves, which leads to a gradually more complicated flow past the model near the surface of the vertical face.

A flow situation typical of moderate values of α and observed at $\beta = 0$ is shown in Fig. 2 ($M_\infty = 2.27$, h = 50 mm, $\alpha = 16°$). In this and the following figures, we have used the following notation: A, B, and C are the lower, vertical, and upper faces; a—a, b—b, etc. are the cross sections of the model and the photographs and flow schemes corresponding to them; 1 and 2 are the projections of plane oblique shock waves from the lower and vertical faces on the surface of faces B and A, respectively (disregarding the interference of these shock waves with each other); I and II are the characteristic segments of the limiting streamlines; D is the diffraction rib; S is the separation line; R is the reattachment line; W is the forward shock wave; the c_i are the inner shock waves; t is the tangential discontinuity.

In the free-diffraction zone, as in the case of an isolated dihedral angle [2], the pressure drop between the upper face and the vertical face of the model causes separation of the stream at the rib of the exterior angle, with the formation of a vortex system over face B. For $M_\infty = 2.27$, the appearance of the vortex is detected at an angle of attack as low as 1°, when the pressure drop at the diffraction rib is $\nu = p_C/p_B \approx 1.06$. Here and hereafter, p_A, p_B, and p_C are the pressures at the surfaces of faces A, B, and C, which are determined from the relations for the oblique shock wave, when α and $\beta > 0$, or for Prandtl—Mayer flow (α and $\beta < 0$). At about $\nu = 1.13$ ($\alpha = 2°$) we see the beginning of the formation of the secondary-separation line S_2, which at $\alpha = 4°$ ($\nu \approx 1.27$) takes on a form typical of separation lines. After this, up to $\alpha = 20°$ the oil-and-carbon-black photographs clearly show the traces of two vortices which rotate in opposite directions and are associated with the separation lines S_1, S_2 and the reattachment lines R_1, R_2. In the immediate vicinity of the diffraction rib there is evidently another vortex, which is provisionally indicated by a dashed curve in a scheme a—a of Fig. 2.

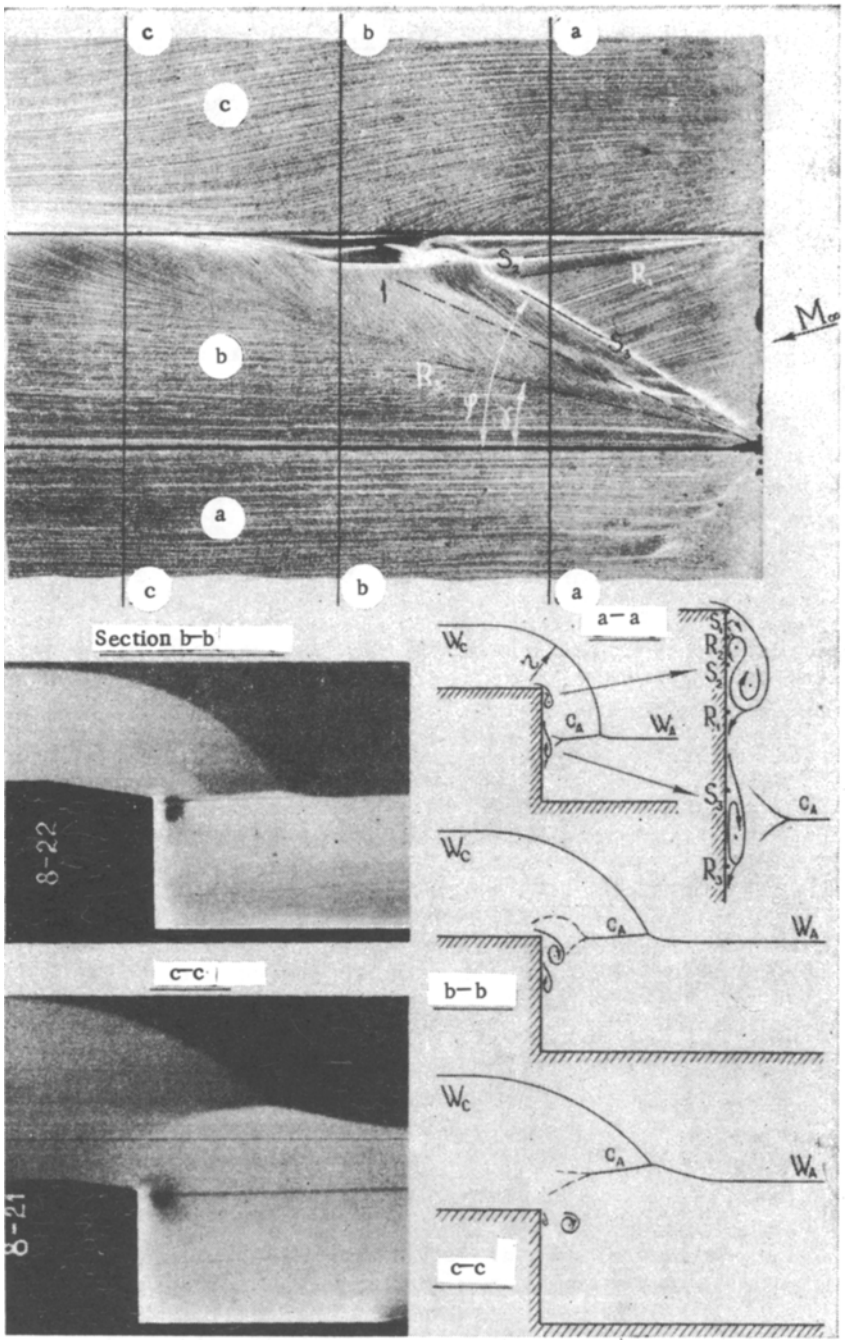

Fig. 2

Visualization of the flow structure by the "laser knife" method, using the scattering of light by microparticles of water, shows that when $M_\infty = 2.27$ and $\alpha = 16°$, the shock wave W_C diffracts into the region of the interior angle along a circle of radius $r \approx 0.95x$, where x is the distance from the leading edge of the model to the section under consideration. Near the leading edge the diffracting shock wave W_C, approaching the surface of the lower face, is gradually attenuated and merges into the curve of small perturbations. The shock wave W_A meets the diffracted shock wave W_C, and as a result of the interaction with it, changes its own configuration.

When the forward shock wave W_A reaches a critical value $\xi^* = p_1/p_B \approx 1.5$, where p_1 is the pressure behind the shock, $p_B \approx p_\infty$), there is a separation of the boundary layer at the surface of the vertical face, which agrees with the data of [12, 14, 16]. In reality, however, this shock wave is caused not by the forward shock wave W_A, as in the case of flow past an isolated interior angle, but by the interior shock wave c_A, which is propagated in the direction of face B from the point at which the jumps W_A and W_C meet (see Fig. 2, a–a). When

TABLE 1

α°	φ°		γ°	
	present study	[16]	present study	[16]
8	22	25,7	—	14,6
12	28	28,9	15	15,2
16	31	33,1	15,5	16,5
20	37	38,7	16,5	18,7

TABLE 2

M_∞	β°	φ°, h, mm			
		12,5	25	50	~200*
2,27	12	No Separation	23	27	28,9
3,0	8	» »	11	18	19,4
	12	5	9,5	18,5	21,4
4,03	8	7,3	9,8	11	14,9
	12	7,5	11,5	13	17,5

*Calculated according to [16].

$M_\infty = 2.27$, the appearance of a developed separation zone bounded by the curves S_3 and R_3 is fixed on the oil-and-carbon-black photographs beginning at $\xi \geqslant 2$ ($\alpha \geqslant 12°$), and for $M_\infty = 4$ at $\xi \approx 1.5$ ($\alpha \geqslant 4°$). This appears to be related to the turbulent or laminar state of the boundary layer at face B for the indicated Mach numbers.

Further downstream, c_A and the separation flow caused by it begin to interact with the vortex system situated near the diffraction rib, as a result of which a λ configuration of the internal jump arises (section b–b). In the region of intensive interaction between c_A and the vortex system, a number of small stagnation zones are formed on the surface of face B, and the care of the main vortex gradually moves away from the surface of the vertical face and becomes a cylindrical vortex filament (section c–c). Simultaneously with this, as the flow develops, the upper and lower branches of the λ shock c_A successively diffract on the rib of the exterior angle, which leads to a substantial increase in pressure and a deviation of the limiting streamlines on the surface of the upper face in the direction opposite the initial position. For moderate values of α and $\bar{x}_h = x/x_h > 1.5$, all the streamlines on the surface of the model become practically parallel to the ribs of the angular configuration, except for a small zone near the diffraction rib. Beginning at $\alpha \geqslant 16°$, we observe on face C a stable picture of the deviation of the streamlines from the diffraction rib, unlike their motion toward the rib in the free-diffraction zone.

On the basis of an analysis of many experimental data for an interior right angle, Zheltovodov [16] obtained, for sufficiently long faces, empirical relations for the angles of inclination φ of the separation lines (drainage of the oil-and-carbon-black mixture) and γ of the reattachment lines of the boundary layer with respect to the direction of the unperturbed stream. Table 1 compares the values of the angles φ and γ for the curves S_3 and R_3 on the surface of face B with respect to the interference rib. As can be seen, the data obtained for $M_\infty = 2.27$, $\beta = 0$, and $h = 50$ mm are somewhat lower than the values calculated from the relations in [16]. As h decreases and M_∞ increases, these relations no longer provide acceptable accuracy in the determination of the angles φ and γ.

2. When $\beta < 0$, the phenomena considered above the aggravated by the presence of a fan of rarefaction waves, which results in an increase of the pressure drops in the investigated zone. A flow situation typical of negative slip angles is shown in Fig. 3 ($M_\infty = 2.27$, $\beta = -12°$, $\alpha = 16°$, $h = 50$ mm).

The vortex system situated in the free-diffraction zone near face B occupies a larger region and is characterized by the appearance of additional separation lines S_3 and reattachment lines R_3 of the stream, which are clearly fixed for pressure drops $\nu \geqslant 4$. In this case we find a five-vortex flow structure (upper part of scheme a–a in Fig. 3). An analogous flow was noted earlier in the case of flow past the lateral face of a dihedral angle near a sharp edge [2].

Unlike the case $\beta = 0$, the separation line S_4 of the boundary layer on face B, arising under the influence of the shock wave from the lower face, has a sharp break approximately halfway up the vertical face. This flow scheme in the front part of the model can be observed most clearly when $M_\infty = 2.27$ and $\beta = -4°$.

The interaction of the shock waves with the vortex system also becomes more complicated. In the first place, W_A, interacting with W_C, which was diffracted by the rib, enters the region of smooth increase in the stream velocity in a fan of rarefaction waves, which is associated with the flow past the vertical face. On the photographs showing the visualization of the flow by the "laser knife" method, the interior shock wave c_A is gradually distorted and, in accordance with the increase in the stream velocity in the investigated zone from M_∞ to M_β,

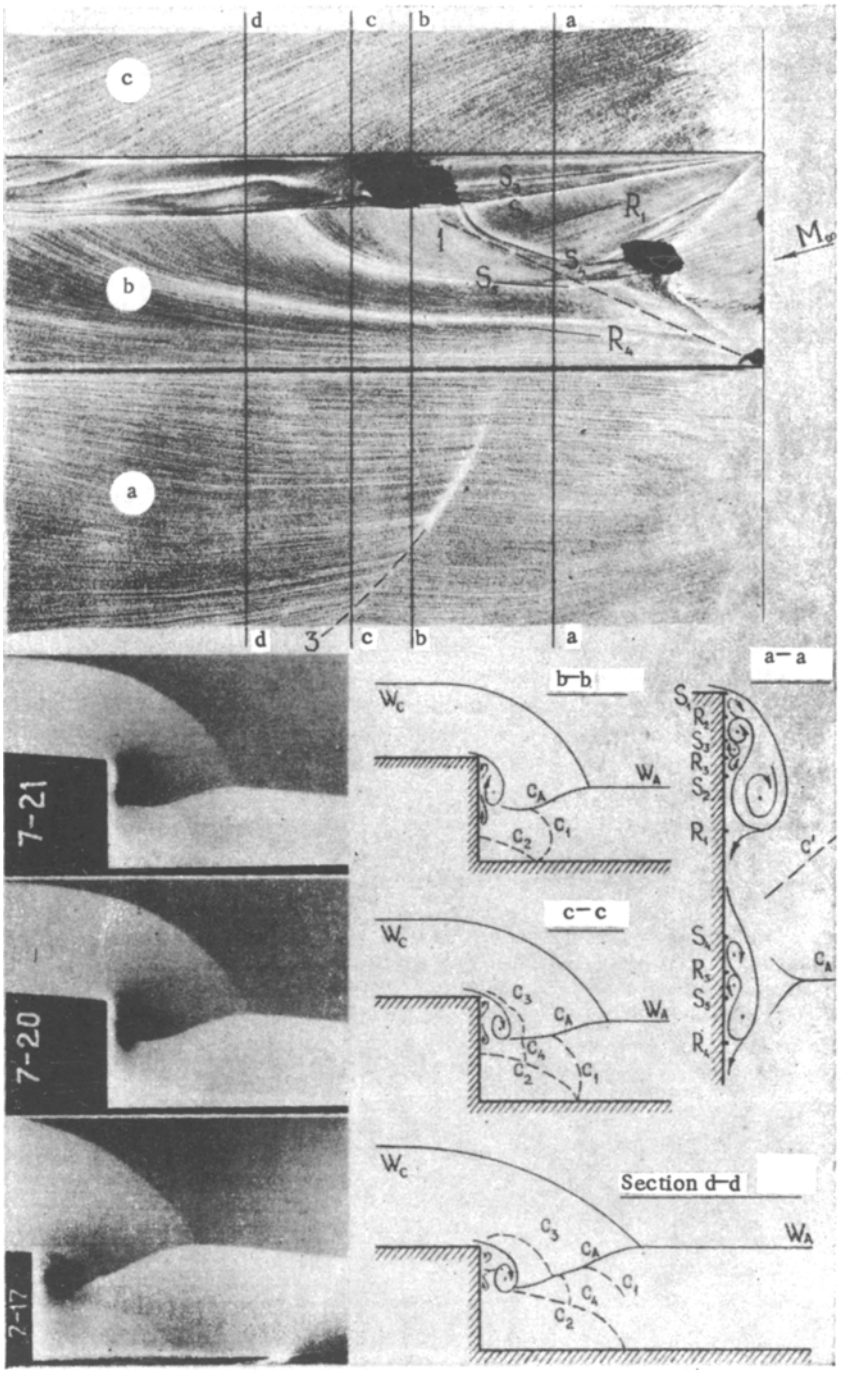

Fig. 3

changes its angle of inclination to the surface of the lower face. The decrease in the compression thickness of the stream (the light-colored zone) under the forward shocks W_C and W_A with movement from left to right is due not to the properties of the flow past the model but to the setting of the "laser knife" plane at an angle β with respect to the leading edge.

In the second place, in the forward part of the model, in the zone affected by the fan of rarefaction waves, there is a suspended shock wave c', which for $M_\infty = 2.27$ and $\beta = -12°$ is inclined to the surface of the vertical face at an angle of about 50°. In regimes with $\alpha \leqslant 0$, as the motion proceeds downstream, c' is displaced in the direction of the lower face and, having reached the surface A, leaves on it a clear arc-shaped trace which is plainly visible on the oil-and-carbon-black visualization photographs. Similar traces on the surface of the lower face are made when $\alpha > 0$ as well. In Fig. 3 this trace is partially indicated by the dashed curve 3.

In the third place, the interior shock wave c_A begins to interact intensively with the vortex system. The separation zone which appeared on the surface of the vertical face under the action of c_A will probably, as in the case $\beta = 0$, work its way under the main vortex and force it away from the surface of the model. On face B there will appear a number of separation curves and stagnation zones, where the oil-and-carbon-black mixture accumulates. While the wind tunnel is shut down, the accumulated drops of this mixture are spread over the surface of the vertical face in the form of extensive dark spots. At a sufficiently large distance from the leading edge ($\bar{x}_h > 3$-4) the vortex system, as in the case $\beta = 0$, becomes a cylindrical vortex filaments, as shown by the oil-and-carbon-black visualization photographs obtained for h = 12.5 and 25 mm.

In the fourth place, in the regime $\alpha > 0$ the interaction between the shocks c_A and c' and between these two and the vortex system is accompanied by the formation of many gasdynamic discontinuities c_i, which are clearly visible on the photographs obtained by the "laser knife" method. In the schemes of Fig. 3 the shocks c_i are indicated by dashed curves, and the figure shows the sequence of their development with displacement in the downstream direction. In this case trace 3 on face A is left by the shocks c_1 and c_2, which form regions of compression of the stream in the vicinity of the interference angle. The substantial increase of pressure in the zone under consideration is evidenced by the increased brightness of the image on the "laser knife" photographs, and also by the data of [24].

With increasing distance from the leading edge, the zone of influence of the interior shocks expands considerably both on face A and on face B. At the same time there appear additional gasdynamic discontinuities c_3 and c_4, which include the vortex system separated from the surface B (see Fig. 3, c–c and d–d).

For $M_\infty = 3$ and 4 and small angles of attack, the intensity of the interior shocks is sufficient to cause separation of the boundary layer that had developed on face A, a fact confirmed by the oil-and-carbon-black visualization of the limiting streamlines.

3. When $\beta > 0$, depending on the ratio of the angles α and β, there are several characteristic types of flow.

At negative or small positive angles of attack, the main contribution to the formation of the flow is made by the vertical face, which in this case is the windward side with respect to the oncoming stream. The flows in the zones of the exterior and interior angles have little effect on each other, and in the first approximation they may be considered insignificant. An example of such flow is shown in Fig. 4 ($M_\infty = 2.27$, h = 50 mm, $\beta = 12°$, $\alpha = 0$). In the regime with $\alpha = 0$ the pressure drop between faces B and C, leading to the formation of the vortex system above the upper face, and the nature of the interaction of the shock wave W_B, whose projection is indicated by curve 2, with the boundary layer of face A depend only on the angle β, which determines the intensity of this shock wave. As β increases, the single-vortex flow is converted to a multivortex flow, which is similar to flow past the zone of free diffraction above the vertical face when $\beta = 0$.

At angles $\beta = 8°$ and $\alpha = 0$, over the entire investigated range of h and Mach numbers, the angles of inclination of the reattachment lines R_1 amount to 5-6°, and when $\beta = 12°$ and $\alpha = 0$, they amount to approximately 7-8°. Similarly, the angles of inclination of the separation lines S_2 with respect to the diffraction rib vary between 3 and 4°. Here the lower values of the angles correspond to $M_\infty = 2.27$, and the upper ones to $M_\infty = 4.03$. The indicated values are close to the data obtained on an isolated exterior right angle.

As β increases, the nonseparation interaction of the shock W_B with the boundary layer of face A becomes a separation interaction. However, owing to the bounded height h of the longitudinal and the flow of gas from the high-pressure zone through the diffraction rib onto face C, the pressure drop on the lower face becomes somewhat smaller than the calculated intensity of the shock wave W_B. Therefore, the value of h has a significant influence on the development of the flow.

This is also evidenced by the stream visualization photographs obtained by the "laser knife" method (Fig. 4, a–a and b–b). As the displacement proceeds in a downstream direction, which in this case is tantamount to a decrease in the relative height of the longitudinal step, we observe a substantial change in the angle of the plane of the shock wave W_B to the surface of face A. For example, whereas at $\bar{x}_h = 0.5$ the shock wave W_B is practically perpendicular to the plane of the lower face, at $\bar{x}_h = 1$ its angle of inclination decreases to about 75°, and the actual interaction of the shock wave with the boundary layer is characterized by the appearance of a λ configuration near the surface A.

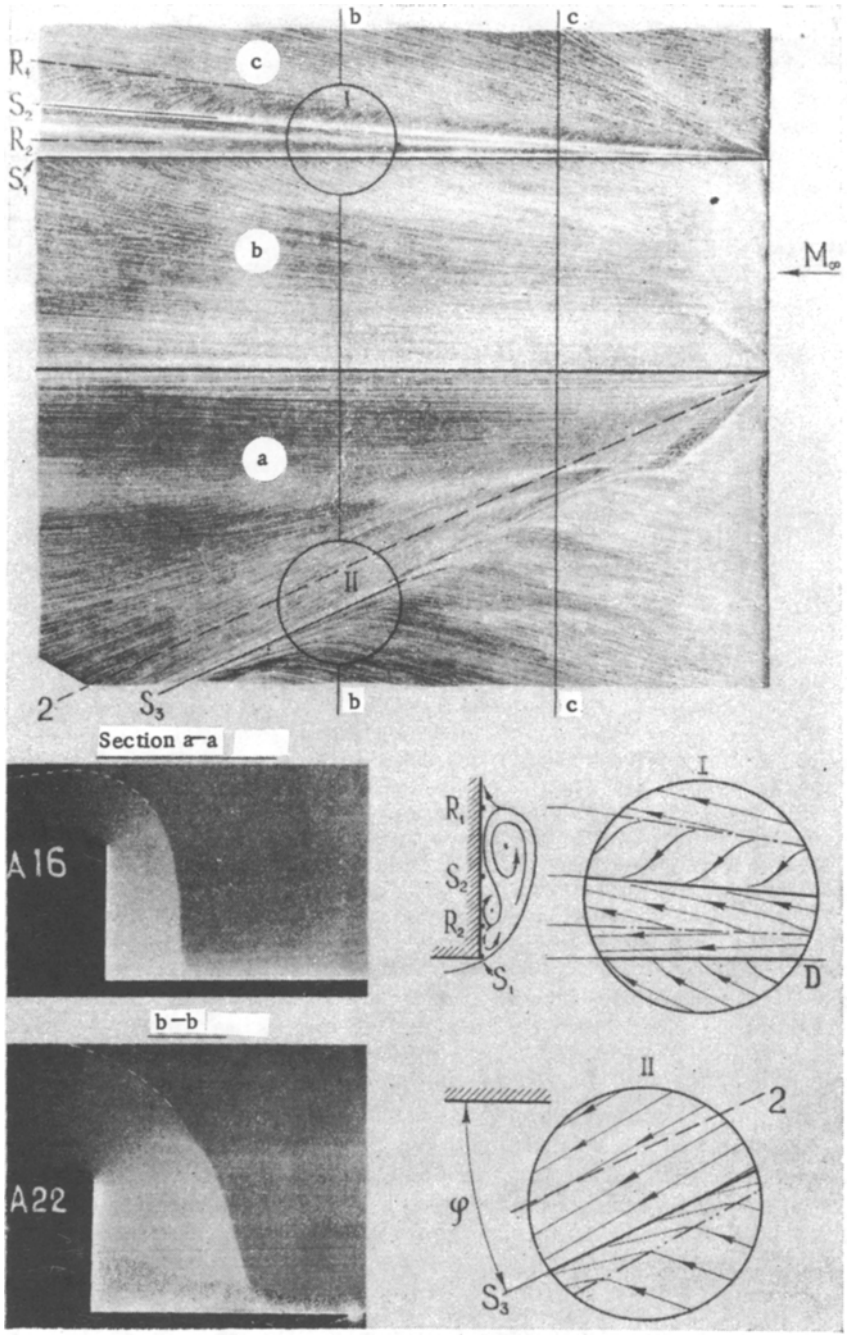

Fig. 4

Table 2 shows the values of the angles of inclination φ of the separation line of the boundary layer naturally developed on face A with respect to the interference rib (scheme II in Fig. 4), obtained for the zone of turbulent flow for various Mach numbers and values of h, as well as the values of φ calculated from the relation in [16]. Here, as in the case $\beta = 0$, this relation becomes inapplicable as the height of face B decreases. It can be seen from Table 2 that as h increases, the values of the angle φ asymptotically approach the data of [16] for an isolated dihedral angle with semi-infinite faces.

For small angles β and large angles α the flow near the vertical face depends to a large extent on the shock waves from faces A and C. At these angles the flow situation is similar to the case $\beta = 0$. As in Fig. 2, a vortex is formed near the diffraction rib above face B, and the shock wave W_A from the lower face leads to separation of the boundary layer on the surface B and transformation of the vertex system. However, owing to the decrease in the relative pressure drops behind the shock waves W_A and W_C in comparison with the pressure on face B, the phenomena considered are less marked than for $\beta = 0$.

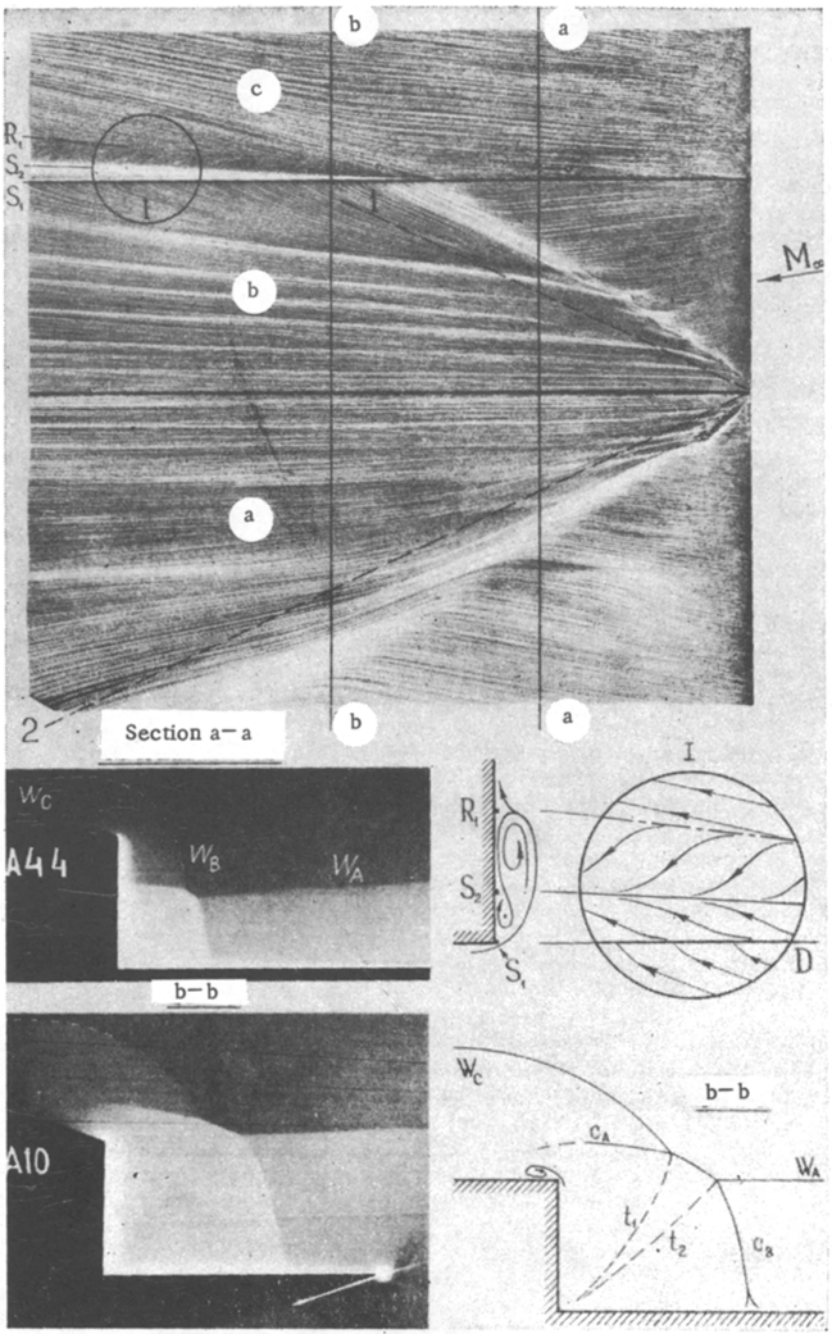

Fig. 5

Another characteristic type of flow takes place in the case $\alpha \approx \beta$, when the region of compression in the zone of the interior angle, as in the case of an isolated dihedral angle, is formed under the combined influence of α and β. In this case the average pressure in the interference region is close to the pressure on a flat plate at an angle of attack $\alpha + \beta$ [11, 24], and therefore the influence of the shock wave W_A on the flow above the upper face is much larger than for $\beta = 0$.

The visualization of the stream by the "laser knife" method shows that in a regime with $M_\infty = 2.27$ and $\alpha = \beta = 8°$ (Fig. 5), as the distance from the leading edge increases, there is a successive irregular interaction between W_A and W_B (section a–a) and between W_A and the shock wave W_C, which in the case of diffraction is joined to W_B (section b–b). This interaction results in the formation of the interior shock wave c_A and c_B and the tangential discontinuities t_1 and t_2. Gradually c_A approaches the exterior angle and diffracts in the direction of the upper face, and this is accompanied by the formation of a vortex near the diffraction rib (Fig. 5, scheme I). As β increases, the vortex system that has developed will become more intensive, and the zone of its influence on face C will expand.

The transition from one flow scheme above the upper face (see Fig. 4) to the other (see Fig. 5) takes place fairly smoothly. In the range from $\alpha \approx 0$ to $\alpha \approx \beta$ we observe an intermediate variety of flow, when the vortex structure above face C occurs near the leading edge, but it is made much stronger by the shock wave c_A, as in the case $\alpha \approx \beta$. All the separation lines and reattachment lines of the stream on face C undergo a substantial break.

Thus, in the case of supersonic flow past a combination of an exterior and an interior right angle there is an essentially three-dimensional mixed interference-diffraction flow. The interference of the shock waves and their interaction with the boundary layers when the height of the vertical face is bounded are accompanied by diffraction of the interior shock waves on the rib of the exterior angle, with the formation of additional vortex systems. The intensive interaction of the shock waves with the vortices formed in the free-diffraction zone above the vertical face leads to the appearance of many gasdynamic discontinuities and the forcing of the vortex filament away from the surface of the model into the external stream. These complicated features of the flows under consideration must be taken into account in the design of calculation model.

The authors are deeply grateful to A. A. Pavlov for participating in the experiments on the visualization of the stream by the "laser knife" method, and also to N. F. Vorob'ev, whose comments had a fruitful influence on the work.

LITERATURE CITED

1. N. F. Vorob'ev, "Problems in supersonic flow past solids of prismatic configuration," Zh. Prikl. Mekh. Tekh. Fiz., No. 5 (1982).
2. V. S. Dem'yanenko and V. P. Fedosov, "Flow of a supersonic stream near a convex dihedral angle," Izv. Sib. Otd. Akad. Nauk SSSR, Ser. Tekh. Nauk, No. 13, Issue 3 (1975).
3. V. P. Fedosov, Calculation of Supersonic Flow Past a Number of Three-Dimensional Angular Configurations within the Framework of the Linear Theory [in Russian], Preprint, Inst. Teor. Prikl. Mekh. Sib. Otd. Akad. Nauk SSSR, No. 27 (1981).
4. C. M. Hung and R. W. MacCormack, "Numerical solution of three-dimensional shock wave and turbulent boundary-layer interaction," AIAA J., 16, No. 10 (1978).
5. C. C. Horstman and C. M. Hung, "Computation of three-dimensional turbulent separated flows at supersonic speeds," AIAA Paper 79-0002 (1979).
6. M. D. Salas and J. Daywitt, "Structure of the conical flowfield about external axial corners," AIAA J., 17, No. 1 (1979).
7. P. Kutler, T. H. Pulliam, and Y. C. Vigneron, "Computation of the viscous supersonic flow over external axial corners," AIAA J., 17, No. 7 (1979).
8. J. S. Shang, W. L. Hankey, and J. S. Petty, "Three-dimensional supersonic interacting turbulent flow along a corner," AIAA J., 17, No. 7 (1979).
9. F. Maconi, "Supersonic, inviscid, conical corner flowfields," AIAA J., 18, No. 1 (1980).
10. M. D. Salas, "Numerical study of flowfields about asymmetric external conical corners," AIAA J., 20, No. 12 (1982).
11. V. S. Dem'yanenko and E. K. Derunov, "Flow of a supersonic stream past a right dihedral angle," Izv. Sib. Otd. Akad. Nauk SSSR, Ser. Tekh. Nauk, No. 8, Issue 2 (1971).
12. V. S. Dem'yanenko and V. A. Igmumnov, "Three-dimensional interaction of a shock wave with a turbulent boundary layer in the region of interference of intersecting surfaces," Izv. Sib. Otd. Akad. Nauk SSSR, Ser. Tekh. Nauk, No. 8, Issue 2 (1975).
13. V. S. Dem'yanenko, "Experimental investigation of the three-dimensional supersonic flow of a gas in the region of interference of intersecting surfaces," Izv. Akad. Nauk SSSR, Mekh. Zhidk. Gaza, No. 6 (1975).
14. A. A. Zheltovodov, "Properties of two- and three-dimensional separation flows at supersonic velocities," Izv. Akad. Nauk SSSR, Mekh. Zhidk. Gaza, No. 3 (1979).
15. A. A. Zheltovodov and A. M. Kharitonov, "Properties of mass and heat exchange in two- and three-dimensional separation flows," in: Materials of the Sixth All-Union Conference on Heat and Mass Exchange [in Russian], Vol. 1, part II, Minsk (1980).
16. A. A. Zheltovdov, "Regimes and properties of three-dimensional separation flows initiated by skewed compression shocks," Zh. Prikl. Mekh. Tekh. Fiz., No. 3 (1982).
17. M. A. Zubin and N. A. Ostapenko, "Experimental investigation of the structure of three-dimensional supersonic flows with separation of the boundary layer at corners," in: Jet and Separation Flows [in Russian], Inst. Mekh. MGU, Moscow (1979).
18. M. A. Zubin and N. A. Ostapenko, "Geometric characteristics of the separation of a turbulent boundary layer when there is interaction with a direct shock wave in conical flows," Izv. Akad. Nauk SSSR, Mekh. Zhidk. Gaza, No. 6 (1983).

19. G. I. Maikapar and A. I. Pyatnova, "Flow of a supersonic stream past the external angle of the shell of an air intake," Uchen. Zap. TsAGI, 11, No. 3 (1980).
20. K. K. Kostyuk, N. A. Blagoveshchenskii, et al., "Experimental investigation of the flow of a stream with high supersonic velocity past a dihedral angle and past the simplest configuration of the 'triangular plate + conical body' type," Tr. TsAGI, Issue 224 (1984).
21. H. Kubota and J. L. Stollery, "An experimental study of the interaction between a glancing shock wave and a turbulent boundary layer," J. Fluid Mech., 116 (1982).
22. D. S. Dolling and S. M. Bogdonoff, "Upstream influence in sharp fin-induced shock wave turbulent boundary layer interaction," AIAA J., 21, No. 1 (1983).
23. V. I. Kornilov and A. M. Kharitonov, "Experimental investigation of a compressed boundary layer near the line of intersection of two plates forming a right angle," Izv. Sib. Otd. Akad. Nauk SSSR, Ser. Tekh. Nauk, No. 8, Issue 2 (1974).
24. M. D. Brodetskii, A. I. Maksimov, and A. M. Kharitonov, "Investigation of interference and diffraction phenomena in supersonic flow past longitudinal steps," in: Aerodynamic Interference in Flow Past Three-Dimensional Bodies [in Russian], Inst. Teor. Prikl. Mekh. Sib. Otd. Akad. Nauk SSSR, Novosibirsk (1980).

FORMATION OF BOUNDARY DISTURBANCES DURING SHOCK-WAVE PROPAGATION IN TUBES MADE OF DIFFERENT MATERIALS

Yu. N. Kiselev, V. A. Klumov,
V. B. Rozhdestvenskii, and V. L. Yur'ev

UDC 533.6.011

The boundary disturbance of the plane front of a shock wave (SW) as it propagates in a tube containing an inert gas was first discussed by Shreffler and Christian [1]. Conducting experiments in which a copper wire was stretched along the axis of a tube, they observed a disturbance of the SW front along the wire. This region of boundary disturbance of the SW had considerable destructive force, propagating with a higher velocity than the main SW, but it radiated with a lower brightness. Such a phenomenon was also investigated in [2, 3]. Conducting experiments in thick-walled tubes, Tsikulin and Popov [2] showed that the presence of the wall, rather than its destruction, as well as the presence of high-energy quanta in the SW emission are important for the formation of boundary disturbances. The vaporization, in advance of the SW front, of material of the tube walls under the action of the SW emission was noted in [3]. The authors of these papers suggested several mechanisms for the formation of a boundary disturbance, but the question of which of them actually occurs remained unresolved. In the present paper this phenomenon is explained on the basis of experiments and the picture of the gasdynamic flow generated is discussed.

In the experiments, a diagram of which is presented in Fig. 1, the SW propagated in a tube 1 filled with xenon at standard density. Flat glass plates 2 with coatings of different materials were placed inside the tube. The SW was generated upon the emergence of a detonation wave at the end of a hexogen charge with a mass of 800 g. A lens of a special shape, made of a mixture of trotyl and hexogen, and used to obtain a plane SW front. The emission from the SW front was recorded by a pyroelectric receiver 3. The generation and propagation of the region of boundary disturbance was recorded with an SFR-2M streak camera in the regime of slit scanning through a violet filter (432 nm) and with a VFU-1 camera in the regime of movie spectrography with a diffraction grating. The SFR-2M camera was also aimed at the side glass window 4 using the system of mirrors 5. The velocity of the central undisturbed part of the SW was measured in a separate test, where the boundary disturbances running ahead of the wave were intercepted by special projections on the tube wall. The SW velocity varied from 7.5 km/sec at the start of the path with a length of 160 mm to 6.5 km/sec at the end. The emission flux density from the front of the undisturbed SW grew from 0 to 4.2 MW/cm^2 in 2.5 μsec, fell to 3.5 MW/cm^2 by 10 μsec, and remained constant up to 25 μsec. The flux density of the radiation acting on the wall varied from 0 to 1.8 MW/cm^2 according to the calculations, while the energy density of the radiation incident on the end of each plate was 8.0,

Moscow. Translated from Zhurnal Prikladnoi Mekhaniki i Tekhnicheskoi Fiziki, No. 1, pp. 116-120, January-February, 1986. Original article submitted November 5, 1984.

0021-8944/86/2701-0103$12.50